N-WASP-mediated invadopodium formation is involved in intravasation and lung metastasis of mammary tumors

Bojana Gligorijevic[1,2,*,‡], Jeffrey Wyckoff[1,*], Hideki Yamaguchi[3], Yarong Wang[1], Evanthia T. Roussos[1] and John Condeelis[1,2,‡]

[1]Department of Anatomy and Structural Biology, Albert Einstein College of Medicine, Bronx, NY 10461, USA
[2]Gruss-Lipper Biophotonics Center, Albert Einstein College of Medicine, Bronx, NY 10461, USA
[3]Division of Metastasis and Invasion Signaling, National Cancer Center Research Institute, Chuo-ku, Tokyo 104-0045, Japan

*These authors contributed equally to this work
‡Authors for correspondence (bojana.gligorijevic@einstein.yu.edu; john.condeelis@einstein.yu.edu)

Accepted 11 November 2011
Journal of Cell Science 125, 724–734

doi: 10.1242/jcs.092726

Summary

Invadopodia are proteolytic membrane protrusions formed by highly invasive cancer cells, commonly observed on substrate(s) mimicking extracellular matrix. Although invadopodia are proposed to have roles in cancer invasion and metastasis, direct evidence has not been available. We previously reported that neural Wiskott–Aldrich syndrome protein (N-WASP), a member of WASP family proteins that regulate reorganization of the actin cytoskeleton, is an essential component of invadopodia. Here, we report that N-WASP-mediated invadopodium formation is essential in breast cancer invasion, intravasation and lung metastasis. We established stable cell lines based on MTLn3 rat mammary adenocarcinoma cells that either overexpressed a dominant-negative (DN) N-WASP construct or in which N-WASP expression was silenced by a pSuper N-WASP shRNA. Both the N-WASP shRNA and DN N-WASP cells showed a markedly decreased ability to form invadopodia and degrade extracellular matrix. In addition, formation of invadopodia in primary tumors and collagen I degradation were reduced in the areas of invasion (collagen-rich areas in the invasive edge of the tumor) and in the areas of intravasation (blood-vessel-rich areas). Our results suggest that tumor cells in vivo that have a decreased activity of N-WASP also have a reduced ability to form invadopodia, migrate, invade, intravasate and disseminate to lung compared with tumor cells with parental N-WASP levels.

Key words: N-WASP, Invadopodia, Breast cancer, Intravasation, Metastasis

Introduction

In primary tumors, cell migration is essential for metastasis (Friedl and Gilmour, 2009; Roussos et al., 2011a; Sahai, 2005). To migrate through barriers carcinoma cells need to remodel extracellular matrix (ECM) (Even-Ram and Yamada, 2005), which is a process controlled by proteases, mainly matrix metalloproteases (MMPs) (Egeblad et al., 2008; Koblinski et al., 2000). In vitro studies have shown that invasive cancer cells, when cultured on components of ECM or basement membranes (collagen I-, fibronectin- and laminin-based substrates) form invadopodia, membrane protrusions specialized to degrade ECM (Buccione et al., 2004). Invadopodia are enriched with a variety of proteins, including actin and actin regulatory proteins, matrix-degrading enzymes, signaling and membrane remodeling proteins. Many of these proteins are present in other structures linked with tumor cell motility but the defining feature of invadopodia comes from their high proteolytic activity. This directly leads to a hypothesis that invadopodia have important roles in one or more steps of the metastatic cascade (Eckert et al., 2011). In addition, invadopodium formation in breast cancer cells is regulated by the epidermal growth factor (EGF) signaling pathway (Yamaguchi et al., 2005a). The EGF receptor (EGFR) and its signaling pathway are also involved in invasion, intravasation and metastasis of breast cancer (Xue et al., 2006).

Intravital imaging studies revealed that carcinoma cells polarize and form protrusions towards blood vessels in primary mammary tumors, which are believed to be involved in invasion and intravasation (Condeelis and Segall, 2003; Sidani et al., 2006; Wang et al., 2002; Yamaguchi et al., 2005b). Additionally, neural Wiskott–Aldrich syndrome protein (N-WASP), has been implicated in cell invasion (Lorenz et al., 2004; Oser et al., 2010; Snapper et al., 2001; Wang et al., 2005; Yamaguchi et al., 2005a).

N-WASP (Miki et al., 1996) is a member of the WASP family of proteins that are key regulators of reorganization of the actin cytoskeleton in several signaling pathways (Stradal et al., 2004; Takenawa and Suetsugu, 2007). N-WASP activates Arp2/3-complex-mediated actin polymerization and this activity is regulated upstream by Cdc42, Nck, Grb2, Src and phosphoinositides. N-WASP was previously shown to be an essential component of invadopodia (Lorenz et al., 2004; Yamaguchi et al., 2005a), but not lamellipodia (Desmarais et al., 2009) or filopodia (Li et al., 2010) in metastatic carcinoma cells. In other cell types present in primary tumors, macrophages are known to develop invasive and adhesive structures very similar to invadopodia (Oser et al., 2011) called podosomes. In these structures the primary controller of actin polymerization is WASP (Linder et al., 1999).

Given this background, we have studied the importance of N-WASP in the invasion and migration of tumor cells in vivo and its requirement for intravasation and metastasis of mammary tumors. In particular, we have studied N-WASP involvement in the formation of invadopodia in vivo in tumor cells and the direct link between invadopodium formation and remodeling of stroma by cancer cells during invasion, intravasation and lung metastasis. We examined the phenotypes of MTLn3 cells with impaired function or silencing of N-WASP, and the ability of these cells to form tumors, invade, intravasate and metastasize. We report that N-WASP-mediated invadopodium formation is necessary for the invasion and intravasation steps in breast cancer metastasis.

Results

Expression DN N-WASP and N-WASP shRNA reduces number of invadopodia and matrix degradation levels

In order to study the role of N-WASP in tumor cell behavior, we established stable MTLn3 rat mammary adenocarcinoma cell lines in which we interfered with the endogenous N-WASP protein. One approach was to overexpress the dominant-negative (DN) form of N-WASP that lacks essential amino acids for activation of the Arp2/3 complex and therefore acts as a competitive inhibitor of endogenous N-WASP proteins as shown previously (Banzai et al., 2000). We also used an alternative approach to block N-WASP activity by silencing N-WASP expression with N-WASP small hairpin RNA (shRNA). The control cells used were parental MTLn3 cells transduced with control vectors (either pMX vector or scrambled shRNA in pSuper vector). All constructs were introduced by retroviral transfections. Immunoblotting analysis demonstrated that DN N-WASP-transfected cells overexpressed ectopic DN N-WASP protein 6.7-fold, whereas N-WASP shRNA resulted in 75% silencing compared with control-shRNA-treated cells (Fig. 1A). All cell lines showed similar morphology and growth rates and no changes in random cell motility were observed (data not shown).

We previously reported that transient interference of N-WASP by siRNA or overexpression of DN N-WASP transfection

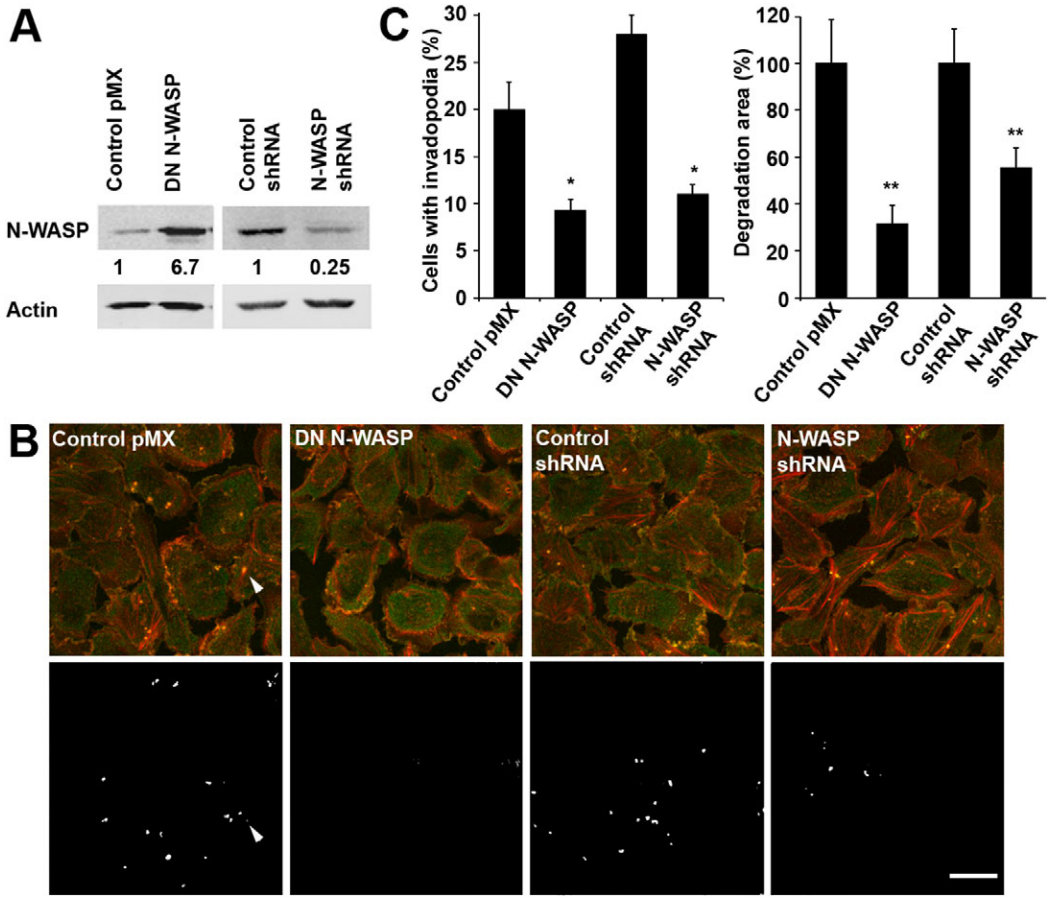

Fig. 1. Establishment of MTLn3 cell lines expressing DN N-WASP and shRNA constructs and effects on invadopodium formation and activity. (**A**) Relative expression levels of N-WASP protein measured in lysates of control MTLn3 (pMX and scrambled shRNA) cells or MTLn3 cells stably overexpressing DN N-WASP or N-WASP shRNA. Immunoblotting was done with anti-N-WASP or anti-β-actin antibodies. (**B**) Representative images of MTLn3 control (pMX and scrambled shRNA) cells and cells expressing DN N-WASP or N-WASP shRNA cultured on a fluorescent gelatin-based matrix. Fixed cells were labeled for anti-cortactin (green) and actin (phalloidin, red). Upper panels show invadopodia (anti-cortactin and phalloidin colocalization – yellow inside cells); lower panels show sites of degraded gelatin substrate (white). Scale bar: 20 μm. The arrowhead points to an invadopodium and its corresponding hole in the matrix. (**C**) The number of cells with invadopodia (dots where cortactin and actin are colocalized) and the percentage of degraded matrix were calculated in control, DN -N-WASP and N-WASP shRNA cell lines. Error bars indicate the s.e.m. of three separate experiments. In each determination, ≥20 different fields of view with ≥100 cells were analyzed; error bars indicate the s.e.m.; *$P<0.05$, **$P<0.01$, Student's *t*-test.

suppressed invadopodium precursor formation in MTLn3 cells in vitro (Oser et al., 2009; Yamaguchi et al., 2005a). The original phenotype was then rescued in vitro by insertion of N-WASP–GFP construct (Yamaguchi et al., 2005a). In the present study we examined the ability of cell lines stably expressing either DN N-WASP or N-WASP shRNA constructs to form mature invadopodia and degrade matrix. Cells were stained for cortactin and actin and colocalization was observed at the cell periphery and in invadopodia as punctate dots, and matrix degradation was present on the ventral surface of the cell (Fig. 1B. upper panels; arrowhead points to an invadopodium). Corresponding images of fluorescent gelatin-based matrix underneath the cells showed degradation (white) patterns that matched the actin–cortactin dots (Fig. 1B, lower panels; supplementary material Fig. S1). Analysis of invadopodium frequency and matrix degradation in images shows that the expression of either DN N-WASP or N-WASP shRNA dramatically reduced the number of cells capable of forming invadopodia and suppressed their proteolytic activity (Fig. 1C). In addition, invadopodia show a decrease F-actin assembly, a result that suggests that the reduction in invadopodium formation occurs through defects in actin assembly [supplementary material Fig. S2 and Desmarais et al. (Desmarais et al., 2009)].

These data lead us to hypothesis that N-WASP-deficient tumor cells are incapable of accomplishing metastatic steps that require invadopodium formation and matrix proteolysis by invadopodia.

N-WASP is required for the MMP-dependent in vivo invasion

Using allograft mammary tumors derived by injecting tumor cells into mammary glands of rats we next examined the invasive ability of tumor cells in an in vivo invasion assay (Fig. 2) (Wyckoff et al., 2000b). Control pMX (empty vector), DN N-WASP, control (scrambled) shRNA and N-WASP shRNA cell lines were injected into mammary glands of rat and grown for 4 weeks (tumors ~1 cm in diameter). As previously described (Wyckoff et al., 2010; Wyckoff et al., 2000a), micromanipulator-guided microneedles containing Matrigel with or without EGF were inserted into the primary tumors, and the number of cells that entered the microneedles was determined. Both DN N-WASP and N-WASP shRNA cells showed a markedly decreased invasive ability in vivo compared with controls. Next, we were interested in whether the invasive ability, which is N-WASP sensitive, was also MMP dependent. If so, a similar defect of invasive ability would be observed by inhibiting MMPs. To this end, we introduced pan-metalloprotease inhibitor GM6001 into the control shRNA tumors. The addition of GM6001 resulted in a significant ($P<0.01$) decrease of the number of cells entering the microneedles (Fig. 2). By contrast, the number of invading cells in control shRNA tumors (with and without dimethyl sulfoxide; DMSO) was not statistically different. These results demonstrate that N-WASP activity is necessary for MMP-dependent in vivo invasion by mammary adenocarcinoma MTLn3 cells, strengthening the hypothesis that N-WASP has a role in early steps of metastasis and that this role is through formation of invadopodia.

Functional N-WASP is required for early steps of metastasis in mouse and rat mammary tumors

In order to test whether N-WASP function is important for tumor metastasis, stable MTLn3 cell lines, all labeled with cytoplasmic (untargeted) GFP, were injected into mammary glands of severe combined immunodeficiency disease (SCID) mice and rats and allowed to form tumors. The mean volumes of DN N-WASP and N-WASP shRNA tumors were not significantly different from those of control tumors ($P>0.25$; data not shown) indicating no change in primary tumor growth. As reported previously, primary tumors derived from control MTLn3–GFP cells spontaneously metastasize to lung and form micro- and macrometastases (Farina et al., 1998; Neri et al., 1982). Therefore, we examined the effects of DN N-WASP and the knockdown of N-WASP compared with controls on tumor metastasis to lung, and whether steps of

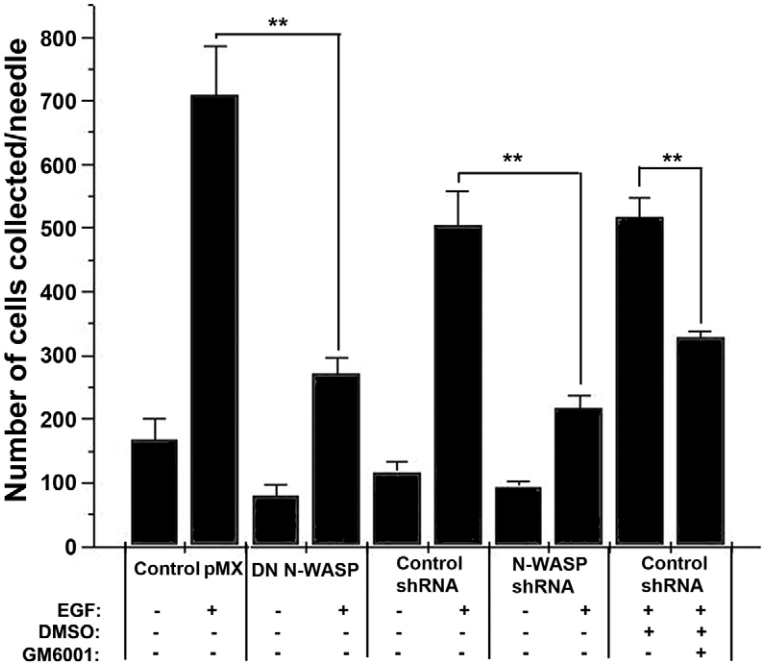

Fig. 2. Tumor cell invasion in vivo in response to EGF requires functional N-WASP. MTLn3 control cells (pMX or scrambled shRNA) or MTLn3 cells stably expressing DN N-WASP or N-WASP shRNA constructs were injected into the mammary glands of rats and formed orthotopic primary tumors. The ability of these cells to invade from primary tumors into microneedles filled with Matrigel with or without (+/–) 25 nM EGF (see Materials and Methods) was measured by counting the cells recovered from the needle after staining with DAPI. In addition, inhibition of invasion in the absence or presence of 10 μM GM6001, an MMP inhibitor, was measured. **$P<0.01$, Student's *t*-test.

dissemination were affected. The number of circulating tumor cells present in blood was determined by collecting blood from the right atrium of the heart, culturing the blood, and later counting the number of tumor cell colonies formed (Wyckoff et al., 2000a) (supplementary material Fig. S3A). This analysis revealed that DN N-WASP and N-WASP shRNA cells have markedly fewer circulating tumor cells than control tumors (Fig. 3A). Moreover, primary tumors derived from DN N-WASP and N-WASP shRNA cells have reduced metastasis to the lungs compared with control tumors (Fig. 3B and supplementary material Fig. S3B). Similar results were seen for both circulating tumor cells and metastasis in SCID mice (Fig. 3C,D). These results indicate that expression of DN N-WASP or the N-WASP inhibits lung metastasis of breast tumors and this may be due to reduced entry into the blood vessel (invasion and intravasation).

To determine whether the role of N-WASP in metastasis is important for dissemination prior to blood vessel entry, control and N-WASP-deficient MTLn3 cells were labeled with the photoconvertible protein Dendra2 (Chudakov et al., 2007). Previously, we reported that the fate of Dendra2–MTLn3 cell populations, when photoconverted from the green to the red state by exposure to 405 nm light, can be followed over days, and dissemination of tumor cells from the primary tumor can be observed directly (Gligorijevic, 2009; Kedrin et al., 2008). Although (red) cells photoconverted in the areas populated with microvessels showed some dispersion and increase in numbers (as a result of cell division) 24 hours later, cells photoconverted in the vicinity of major blood vessels showed a significant ($P=0.012-0.028$) decrease in cell numbers 24 hours later. Here we used this assay on both control tumors and N-WASP-deficient tumors in order to directly compare their abilities to intravasate. Squares of 250×250 μm next to or around major blood vessels were photoconverted at 0 hours, and three-dimensional (3D) image stacks were collected at 0 hours and 24 hours (supplementary material Fig. S4). The number of red cells in the control tumors decreased by 14–37% over 24 hours, which was shown previously to be due to dissemination of cells by the blood stream (Kedrin et al., 2008; Roussos et al., 2011b), there was a slight increase (due to cell division) or no change in the number of red cells in DN N-WASP and N-WASP shRNA tumors (Fig. 4). This result further suggested an important role for N-WASP in the early steps of metastasis by invasion and intravasation. Combined with the data from cells cultured on thin matrices and the in vivo invasion assay, these results suggest that the formation of invadopodia in vivo is N-WASP sensitive and directly involved in tumor cell migration through the tissue and intravasation.

N-WASP function is required for cell protrusion and migration in vivo

In order to directly assess the role of N-WASP in cell motility within primary tumors, multiphoton intravital imaging of GFP-labeled tumors (pMX, DN N-WASP, control shRNA and N-WASP shRNA) was performed following skin flap surgery (Farina et al., 1998; Wang et al., 2002). Tumor cells with suppressed N-WASP were rounded and less polarized than cells with parental levels of N-WASP (Condeelis and Segall, 2003) in the living tumors (Fig. 5). As previously described, cells with parental N-WASP levels are often motile (Fig. 5A) and form protrusions (Fig. 5B), in contrast to tumor cells deficient in N-WASP.

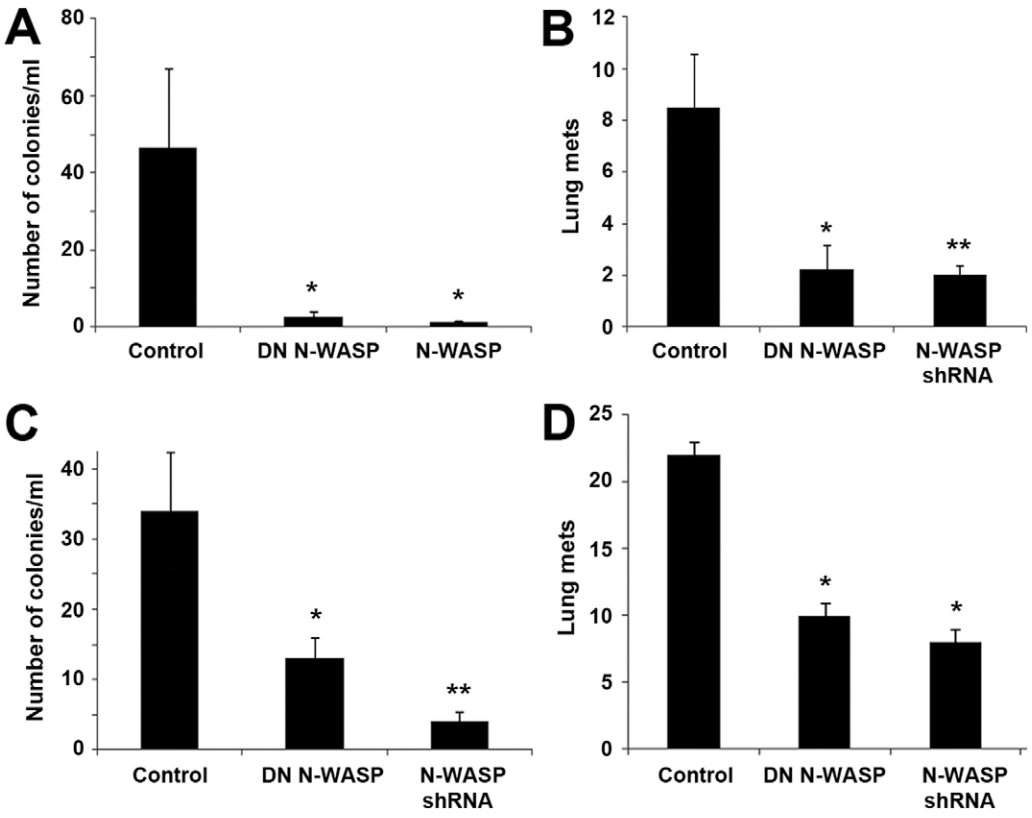

Fig. 3. The presence of circulating tumor cells and formation of lung metastasis requires N-WASP in rat and mouse mammary tumors. (**A**,**B**) Rat tumor-cell-derived mammary tumors in rat. (A) Number of viable circulating tumor cells per milliliter of blood; (B) Number of lung micrometastases. (**C**,**D**) Rat tumor-cell-derived mammary tumors in SCID mice. (C) Number of viable circulating tumor cells per milliliter of blood; (D) number of lung metastases. Error bars indicate the s.e.m.; *$P<0.05$, **$P<0.01$, verified by Mann–Whitney test.

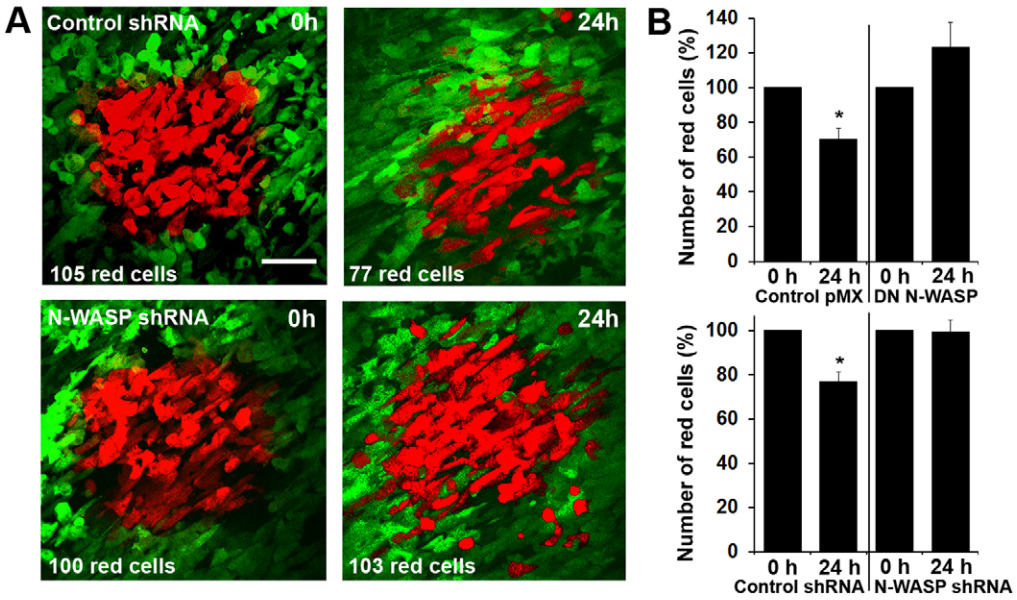

Fig. 4. Intravasation of tumor cells in the primary tumor requires N-WASP. (**A**) At 0 hours, a region of cells was photoconverted (red) in highly vascular regions of the tumors grown from either Dendra2–control-shRNA MTLn3 (top) or Dendra2–N-WASP-shRNA MTLn3 (bottom). At 0 hours and 24 hours *z*-stacks of 0–100 μm were collected in the green and red channels, and maximum projections are shown. This intravasation assay documents that there is less movement of tumor cells into blood vessels from tumors derived from Dendra2–N-WASP shRNA MTLn3 cells. Scale bar: 70 μm. (**B**) Number of red tumor cells remaining around blood vessels when normalized to the number at 0 hours. Measurements were based on three or four animals per cell line, 5–11 regions per animal. Error bars indicate the s.e.m. *$P<0.05$, Student's *t*-test.

Tumor cell motility was then monitored in 3D by time-lapse imaging (over 30-minute periods). Fig. 5A show stills from representative time-lapse images where dots point to the cell front (yellow at 0 minutes, red at 30 minutes) and arrows indicate the cell trajectory. In N-WASP-deficient tumors, there was a dramatic decrease in motile cells compared with control tumors (Fig. 5C). The few motile cells in the N-WASP-deficient tumors had a similar speed and directionality as the control cells (Fig. 5D,E). In addition, protrusions seen forming in control tumors (Fig. 5B) were absent from N-WASP-deficient tumors (Fig. 5B,E), demonstrating that some of the protrusion formation in vivo was N-WASP dependent. Because the N-WASP-deficient cells are unable to form invadopodia, we hypothesized that some of the protrusions seen in vivo are invadopodia and that the lack of proteolytic activity associated with invadopodia is essential for extracellular matrix remodeling and cell migration through the tissue. Our next step was, therefore, to test whether N-WASP-dependent protrusions in tumors cells in vivo have structural components typical for invadopodia and whether they are linked to proteolytic activity of tumor cells.

N-WASP-sensitive protrusions observed in tumors have structural components and proteolytic activity typical for invadopodia

Invadopodial assays, such as the one used in Fig. 1B, commonly consist of detecting enrichment of essential structural invadopodium markers and colocalized proteolysis of a fluorescent substrate such as fibronectin, gelatin or collagen. They have become a standard technique for cell cultures grown on thin matrices, but standardized invadopodial assays for 3D cell culture or tumor tissue (ex vivo and in vivo) have not been established yet. Previously, quenched substrates and immunofluorescence have been used to show areas of matrix proteolysis (Fisher et al., 2009; Packard et al., 2009; Sloane et al., 2006) in 3D culture, whereas proteolysis in tissue sections has been visualized by in situ zymography (Frederiks and Mook, 2004). To compare levels of proteolytic degradation in control and N-WASP-suppressed tumor cells, we applied an antibody against degraded collagen, Collagen 3/4 (i.e. Col2 3/4 short), which recognizes collagen fragments created by the proteolytic activity of MMP-1, MMP-2 or MMP-13 (Tolde et al., 2011; Wolf et al., 2007) in tumor cryosections (Fig. 6A). Results were confirmed by direct comparison of the proteolysis detected as the absence of gelatin (supplementary material Fig. S5A) and association with cortactin as a structural invadopodium marker (supplementary material Fig. S5B). When combined with DAPI, cortactin and actin, the Collagen 3/4 antibody indicated the presence of invadopodial protrusions in cells adjacent to the tumor edge or tumor blood vessels (invasive edge areas, Fig. 6B, and perivascular areas, Fig. 6C; also supplementary material Fig. S6). In cryosections of N-WASP-deficient tumors there was only one third of the number of invadopodia compared with control sections, which is similar to the results of in vitro cultures. However, the degraded area in N-WASP-deficient tumors was approximately one-tenth than in control tumors whereas in the in vitro experiments there was an approximately one third than in control tumors.

Finally, we tested whether the N-WASP is localized to invasive protrusions and, therefore, whether it has a direct function in invadopodium assembly in tumor cells in vivo, followed by matrix degradation. To this end, we sectioned tumors from MTLn3 cells expressing Cerulean-labeled N-WASP (Cerulean–N-WASP–MTLn3). Fig. 7A shows cell protrusions, aimed towards an adjacent blood vessel (white

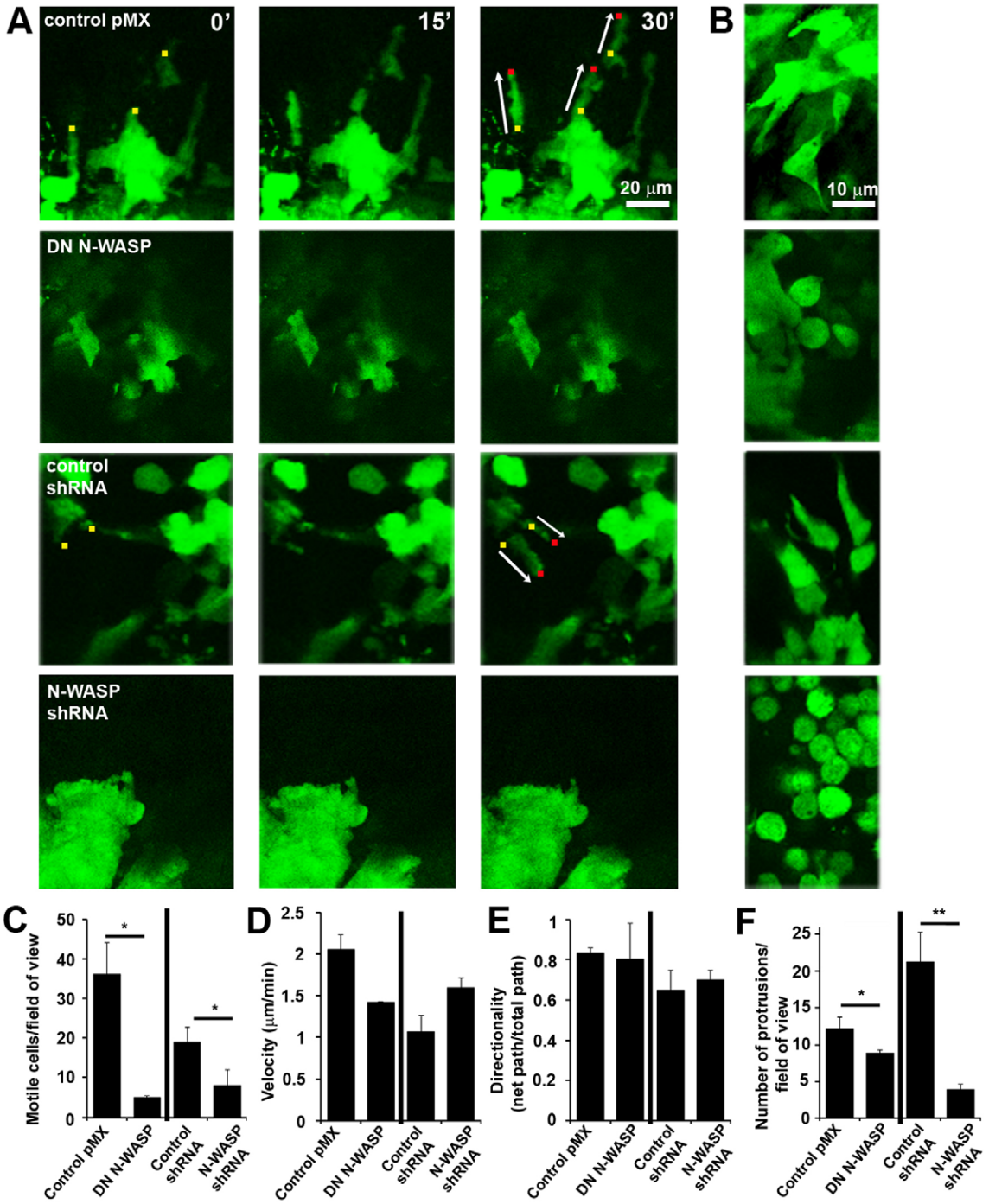

Fig. 5. Cell motility and protrusion formation in vivo requires N-WASP. (**A**) Motility of control and N-WASP-deficient GFP-labeled cells was monitored over time at different regions of the tumor using time-lapse images taken at 0, 15 and 30 minutes (images at same z-sections are shown). Small colored squares indicate the cell fronts (yellow at 0 minutes, red at 30 minutes) and arrows show the length of the trajectory of the migrating cells. (**B**) Higher magnifications of regions where cells are sparsely distributed showing that more protrusions are present in control tumors. (**C**–**F**) Data from both control and N-WASP-deficient tumors showing the number of motile cells per 4D stack (C), velocity of motile cells (D), directionality of motile cells (E) and number of protrusions per 4D stack (F). *$P<0.05$, **$P<0.01$, Student's *t*-test, from three or more different tumors. The 4D stacks were $512 \times 512 \times 100$ μm $\times 30$ minutes; $n=30$.

dashed line) that are enriched in cortactin, actin and N-WASP (Fig. 7B). Further quantification of >15 protrusions showed similar levels throughout the tissue (Fig. 7C). Finally, supplementary material Fig. S7 demonstrates that degradation of collagen I occurs around protrusions rich in cortactin, actin and N-WASP.

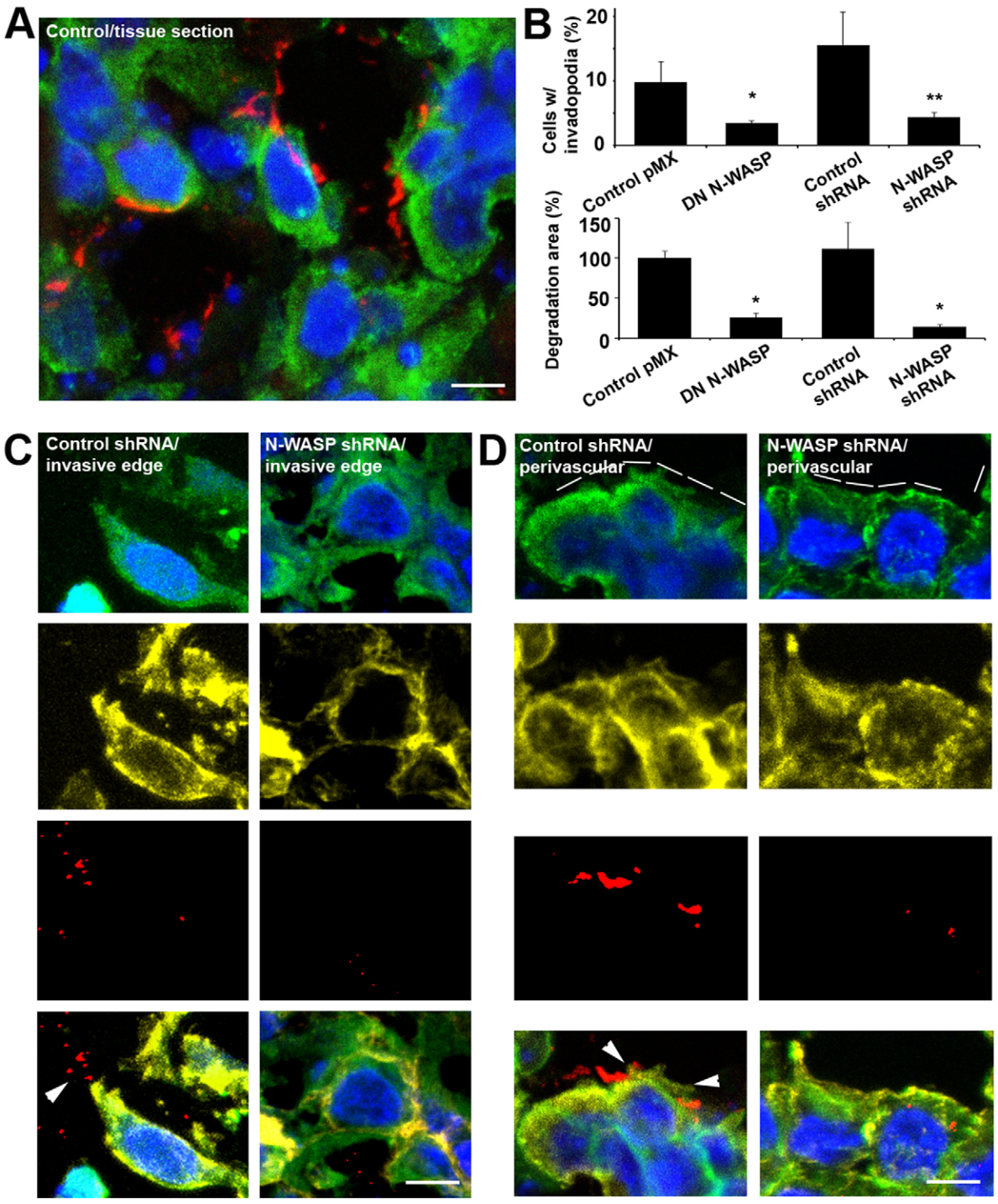

Fig. 6. N-WASP-sensitive protrusions observed in tumors contain invadopodium markers and have degradation activity. (**A**) Matrix degradation sites detected by immunofluorescence (Collagen 3/4; red) in control shRNA tissue slices (anti-cortactin, green; DAPI, blue). Scale bar: 10 μm. (**B**) Quantification of the average number of protrusions, and collagen-I-degraded area in control tumors, DN N-WASP and N-WASP-shRNA tumors, as determined with the Collagen 3/4 assay. *$P<0.05$, Student's *t*-test. (**C**,**D**) Immunohistofluorescence of control shRNA tumors and N-WASP shRNA tumors in (C) the invasive edge and (D) areas next to major blood vessels (perivascular). DAPI is blue, anti-cortactin is green, phalloidin is yellow, Collagen 3/4 is red. The bottom row of images are merged images of all the markers. White arrowheads point to protrusions associated with degradation activity. Scale bars: 10 μm.

Discussion

Breast cancer metastasis is the sum of multistep processes, including migration and invasion through tumor stroma, intravasation inside the primary tumor, tumor cell dissemination, extravasation and cell growth at the secondary sites. Our data demonstrates that N-WASP activity is essential for the formation of proteolytic protrusions (invadopodia) in vivo, which in turn drive the invasive steps of metastasis. Silencing of

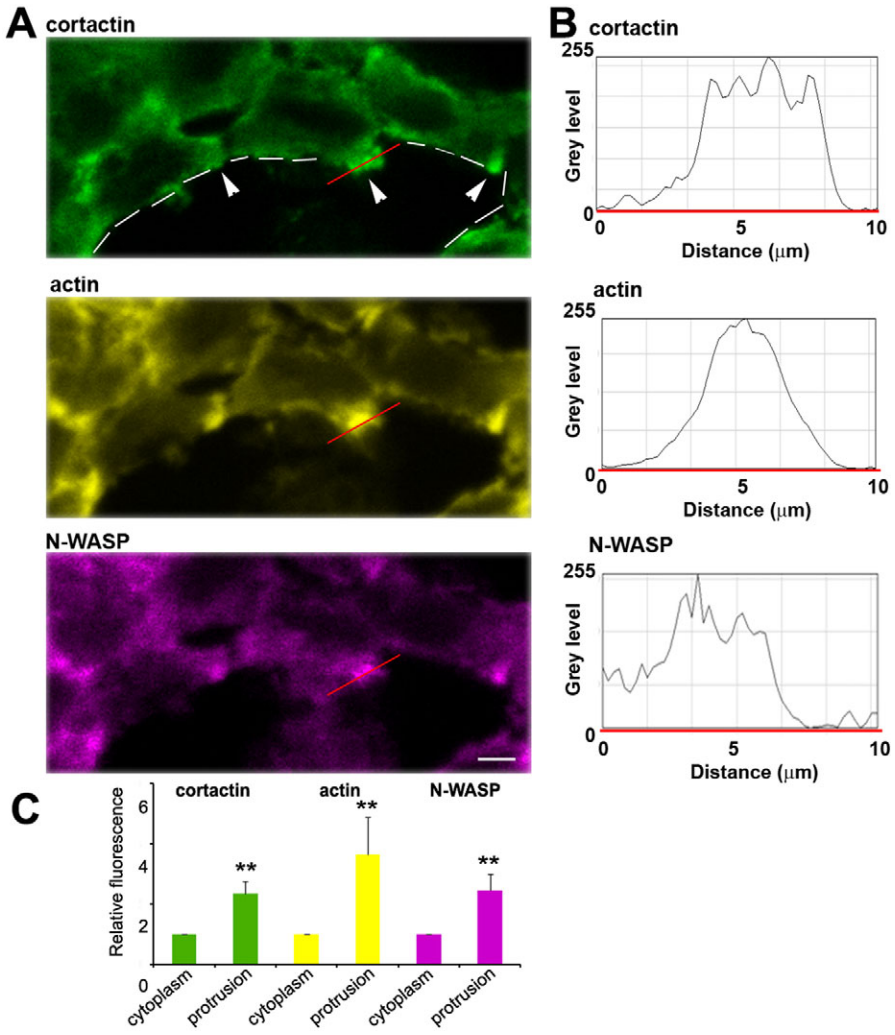

Fig. 7. Protrusions observed in tumors are enriched in actin, cortactin and N-WASP. (**A**) Cerulean–N-WASP–MTLn3 tumor sections (purple) in the area next to a blood vessel (dashed white line), additionally stained by anti-cortactin (green) and phalloidin (yellow). Scale bar: 7 μm. (**B**) Intensity profiles of cortactin, actin and N-WASP along the red line shown in A illustrating enrichment of these proteins in the protrusion. (**C**) Levels of cortactin (green), actin (yellow) and N-WASP (purple) in protrusions relative to the average cytoplasmic levels illustrating enrichment of these proteins in protrusions in Cerulean–N-WASP–MTLn3 tumors. Error bars indicate the s.e.m. for >15 protrusions; $^{**}P<0.01$, Student's *t*-test.

N-WASP was shown to substantially reduce the formation of invasive protrusions, and consequently invasive migration in vivo, intravasation, the number of circulating tumor cells and metastasis to the lungs.

Invasive migration was reduced to a similar level in tumors deficient in N-WASP and when using an MMP inhibitor. These results show that N-WASP-sensitive migration in tumors is MMP-dependent but it also implicates a possible feedback loop in invasive cell migration. Several studies have suggested the possibility of an invadopodial cycle (Magalhaes et al., 2011) in which the assembly of invadopodial proteins (cortactin, N-WASP, cofilin, etc.) is the first and MMP proteolysis is the last stage in the cycle (Oser et al., 2009), and the feedback signals (Clark et al., 2007) initiate a new cycle to extend invadopodia further into the matrix. If this is the mechanism of invadopodial extension, breaking the cycle either by inhibiting assembly of proteins or by MMP inhibition should result in a similar phenotype.

Detachment of cancer cells from primary tumors requires loss of cell–cell adhesion and enhanced cell motility. It is unclear whether N-WASP functions in this process. A previous study has shown that the overexpression of N-WASP or DN N-WASP does not affect cell–cell junctions in epithelial cells (Yamaguchi et al., 2002) and that DN N-WASP overexpression had little effect on random cell migration in vitro, indicating that N-WASP is not involved in general cell locomotion. A different study (Martin et al., 2008) reported that N-WASP overexpression increased adhesiveness in breast cancer cells and reduced tumor growth rate.

To intravasate, carcinoma cells need to break down basement membrane and the endothelial barrier surrounding blood vessels. It has been shown that upregulation of EGFR and its sensitivity to EGF (Roussos et al., 2011b) is closely correlated with enhanced intravasation and lung metastasis of breast tumors (Xue et al., 2006). We also reported that EGFR signaling is essential for invadopodium formation in MTLn3 cells and that N-WASP is an essential mediator of invadopodium formation downstream of EGFR signaling (Oser et al., 2009; Yamaguchi et al., 2005a). Therefore, it is probable that EGF-stimulated formation of invadopodia promotes carcinoma cell intravasation. This is supported by our observations here and those obtained by intravital imaging previously that carcinoma cells around blood vessels form vessel-directed protrusions before they intravasate (Condeelis and Segall, 2003; Wang et al., 2002; Yamaguchi et al., 2005b). In this study, we found that perturbing the function of N-WASP by either a dominant negative construct or shRNA

inhibits invadopodium-mediated ECM degradation and in vivo invasion, as well as the formation of protrusions, by carcinoma cells. These results, together with our previous studies, strongly suggest that N-WASP-mediated invadopodium formation is specifically involved in the invasion and intravasation steps of tumor metastasis.

It is well established that WASP family proteins, including WASP, N-WASP and WAVE1, 2 and 3, are key regulators of actin polymerization, during cell migration and invasion (Takenawa and Suetsugu, 2007). WAVE proteins regulate the formation of lamellipodia that determine cell direction and protrusive force for general cell migration. It has been previously reported that WAVE2 knockdown in mammary adenocarcinoma and melanoma cells blocks formation of lamellipodia in vitro and lung metastasis in experimental metastasis assays, respectively (Kurisu et al., 2005; Sarmiento et al., 2008). Additionally, the expression level of WAVE2 protein is increased as melanoma cells become metastatic (Yamaguchi and Condeelis, 2007). These results strongly suggest that WAVE2-mediated cell migration is necessary for cancer cells to acquire a metastatic potential.

In contrast to WAVE proteins, N-WASP regulates the formation of more specialized protrusions such as invadopodia, which degrade ECM (Li et al., 2010; Yamaguchi et al., 2005a). Our data agree with those of Li et al., who showed that siRNA N-WASP knockdown reduces collagen I degradation by ~60% (Li et al., 2010). In addition, the total number of protrusions in N-WASP-deficient fibroblasts from N-WASP null embryos is substantially reduced (Snapper et al., 2001). Carcinoma cells overexpressing DN N-WASP have no obvious defect in lamellipodium formation and random cell migration in vitro (data not shown), confirming that N-WASP is not involved in general cell migration driven by lamellipodial protrusions. However, N-WASP-dependent invadopodium assembly has been implicated in chemotaxis to EGF in tumor cells (Desmarais et al., 2009), and WASP is required for both podosome assembly and chemotaxis by macrophages (Zicha et al., 1998), suggesting that N-WASP- and WASP-dependent invasive protrusions are involved in directional migration toward growth factors. These results are consistent with our observations that N-WASP-dependent protrusions that extend toward blood vessels are correlated with intravasation and metastasis.

It has been reported that lower levels of expression of N-WASP in whole breast tumor tissue is correlated with poor outcome, using disease-free survival as the end point (Martin et al., 2008). However, this study did not evaluate the behavior of the migratory and disseminating population of breast cancer cells in the primary tumor or the requirement of N-WASP for these phenotypes in vivo. It is not clear whether the lower levels of N-WASP expression were confined to the migratory tumor cells. Our results indicate that the invasive and migratory population of tumor cells in vivo requires N-WASP for migration, intravasation and metastasis.

Taken together, all of the above cited studies establish that WASP-family proteins have distinct roles in cell migration during tumor invasion and metastasis: WAVE proteins regulate lamellipodium-mediated general cell migration and N-WASP regulates invadopodium-mediated directional cell migration through stroma and toward blood vessels, which requires matrix remodeling. In conclusion, the potential of N-WASP as a target for anti-invasion and anti-metastasis therapeutics should be investigated further.

Materials and Methods

Establishment of stable cell lines

MTLn3 cells derived from rat mammary adenocarcinoma (Neri et al., 1982), which are a basal breast cancer cell type (Roussos et al., 2011b), were cultured and maintained in α-MEM supplemented with 5% FBS and antibiotics as described previously (Neri et al., 1982; Segall et al., 1996). A control pMX cell line was created by infection of MTLn3 cells stably expressing GFP (Farina et al., 1998) with a pMX virus. To generate DN N-WASP, the same cells were infected with pMX retrovirus containing DN N-WASP cDNA. A control for N-WASP knockdown (control shRNA), was created by infection of MTLn3 cells with pSuper retrovirus expressing scrambled shRNA (TCCACACCACTACACGAGC) (Gevrey et al., 2005). To generate N-WASP knockdown cells (N-WASP shRNA), MTLn3 cells were infected with pSuper retrovirus expressing shRNA targeted to rat N-WASP cDNA (GACGAGATGCTCCAAATGG-TTCAAGAGA-CCAT-TTGGAGCATCTCG-TC) (Yamaguchi et al., 2005a).

Cerulean–N-WASP–MTLn3 cells were a gift from Ved Sharma (Albert Einstein College of Medicine, NY). Dendra2-expressing cell lines (control pMX, control shRNA, DN N-WASP and N-WASP shRNA) were generated by transfecting cells with Dendra2 using Lipofectamine 2000. Retroviruses were expanded by transfection in Phoenix packaging cells. Under these conditions, >95% of cells were infected with the stably expressing or knockdown N-WASP.

Invadopodia assay, immunofluorescence and immunohistofluorescence

Counting of invadopodia and analysis of the degradation area in cell culture was performed as described previously (Yamaguchi et al., 2005a). Briefly, cells were cultured on Alexa-Fluor-568–fibronectin-coated or Alexa-Fluor-405–gelatin-coated coverslips for 8–16 hours, fixed in 3.7% formaldehyde for 15 minutes and permeabilized with 0.1% Triton X-100 for 10 minutes. Measurement of degradation area in tumors was performed on frozen tissue slices. Tumors grown in SCID mice were excised and lightly fixed (1 hour in 3.7% paraformaldehyde), washed for 1 hour in cold PBS and dehydrated overnight in 30% sucrose. They were then embedded in OCT and 6 μm sections cut using a cryostat. Sections were permeabilized using 0.1% Triton X-100 or cold acetone for 10 minutes.

Cultures or tissue slices were blocked in 1% BSA and 1% FBS for 1 hour, incubated with primary antibodies that were diluted in blocking buffer for 1 hour, and then with Alexa-Fluor-conjugated secondary antibodies diluted in blocking buffer (Invitrogen; 1:300) mixed with Alexa Fluor 488, 543 or 633 and/or Alexa-Fluor-633–phalloidin (Invitrogen; 1:300) for 1 hour. Primary antibodies used were against cortactin (Abcam ab-33333; 1:100) or degraded collagen (Ibex Pharmaceuticals, C1 C2 antibody or Col2 3/4 short antibody, 1:100; we refer to this antibody as Collagen 3/4). In addition, tissue samples were incubated with DAPI for 10 minutes. Cells were observed with an Olympus widefield microscope equipped with a cooled charge coupled device (CCD) camera, or with a Leica SP5 confocal laser-scanning microscope. ImageJ was used for image processing and quantification of invadopodial degradation areas. Briefly, 3D stacks (0–5 μm) of images of degraded fluorescent gelatin or degraded collagen staining were combined into a maximum projection, processed using the smoothing filter and thresholded to the top (or bottom) 20% of the signal (supplementary material Fig. S1). Processing removes heterogeneities in matrix thickness and brightness and nonspecific antibody binding and delineates degradation borders. In addition, gelatin matrix images were inverted (black to white) for easier comparison with antibody labeling.

In vivo invasion, circulating tumor cells and lung metastases

All procedures involving animals were conducted in accordance with NIH regulations, and approved by the Albert Einstein College of Medicine Animal Use Committee.

MTLn3 cells (control pMX, control shRNA, DN N-WASP and N-WASP shRNA) were injected into the mammary glands of 7-week-old female Fischer 344 rats or 5- to 7-week-old SCID mice and allowed to form tumors for 4–5 weeks. The in vivo invasion assay with MTLn3-derived mammary tumors in rats was performed as described previously (Wyckoff et al., 2000b). In brief, the in vivo invasion assay uses microneedles filled with Matrigel and growth factor (EGF) to collect the invasive tumor cells from primary tumors. Microneedles were held in a clamping devise and positioned in the primary tumor with a micromanipulator. Cells were collected over 2.5–4 hours and animals were anesthetized with 2–5% isoflurane throughout. The number of tumor cells collected was counted on a widefield microscope after expelling them on a glass slide and incubating them for 10 minutes with DAPI.

Circulating tumor cell count was determined as described previously (Wyckoff et al., 2000a; Roussos et al., 2011b). Briefly, 1–2 ml blood was drawn from the right ventricle of anesthetized mice and plated in α-MEM. Following 7 days in cell culture, tumor cells and/or cell colonies were counted and calculated as the number of circulating tumor cells surviving per milliliter of drawn blood. All cells counted were GFP positive, confirming their identity as tumor cells (supplementary material Fig. S3A). After blood was drawn from the rats and mice they were killed and the lungs were removed. The number of micrometastasis on and near the surface of the lungs were counted in twenty random fields using a 60× objective

on a widefield microscope (supplementary material Fig. S3B). Tumor size was determined after excision as an average of the *x*-, *y*- and *z*-dimensions.

Multiphoton Intravital Imaging

Multiphoton imaging of GFP-labeled tumors was done as described previously (Wyckoff et al., 2010). Briefly, GFP-labeled MTLn3 (control pMX, control shRNA, DN N-WASP and N-WASP shRNA) were injected into the mammary fat pads of 5- to 7-week-old SCID mice. After 4–5 weeks, skin flap surgery was performed on anesthetized animals. The exposed area of the tumor was positioned on top of a coverslip on an inverted microscope and imaged using an Olympus FV1000-MPE multiphoton system with 880 nm excitation. Cell velocity and directionality were calculated using a custom-written ROI tracking ImageJ plugin (Entenberg et al., 2011).

In vivo Intravasation assay

The mammary imaging window implantation and photoconversion of constitutively expressed Dendra2 was performed as described previously (Gligorijevic et al., 2009; Kedrin et al., 2008). Briefly, Dendra2-expressing MTLn3 cells (control pMX, control shRNA, DN N-WASP and N-WASP shRNA) were injected in SCID mice. A window was implanted on top of the growing tumor after 17–20 days (5–7 mm in diameter). Following a 3-day recovery, the mouse was anesthetized and placed in an imaging box (Gligorijevic et al., 2009). Photoconversion was done by exposing a 250×250 µm square to 405 nm laser light using a Leica SP5 confocal system with a $20\times$ objective. Photoconversion sites were chosen to be either far from (>200 µm) or close (<10 µm) to a major blood vessel. All further imaging was done using a custom-built multiphoton system, which contained two Ti-Sapphire lasers and an inverted Olympus IX71 microscope (Entenberg et al., 2011). Lasers were tuned to 880 nm (for imaging of the green species of Dendra2) and 1035 nm (for the red species of Dendra2) (Kedrin et al., 2008). All photoconversion sites were imaged at 0 hours and 24 hours post-photoconversion, collecting 3D image stacks 0–100 µm from the tumor surface. The number of photoconverted Dendra2 cells was counted in five 20-µm-thick *z*-sections (supplementary material Fig. S4) using the ROI plugin for ImageJ (Entenberg et al., 2011).

Acknowledgements

We are grateful to Ved Sharma, Dianne Cox and Jose Javier Bravo for gifts of cell lines and constructs. We thank all members of the John Condeelis, Jeffrey Segall and Dianne Cox laboratories and the Analytical Imaging Facility at Albert Einstein College of Medicine for helpful discussions.

Funding

This work was supported by National Institutes of Health [grant number CA150344 to H.Y., E.R. and J.C.]; National Institutes of Health [grant number CA100324 to J.W. and Y.W.]; National Institutes of Health Mouse Models of Human Cancers Consortium [grant number UO1-1105490 to J.C.]; and a Charles H. Revson Fellowship in Biomedical Science 2010 to B.G. Deposited in PMC for release after 12 months.

Supplementary material available online at
http://jcs.biologists.org/lookup/suppl/doi:10.1242/jcs.092726/-/DC1

References

Banzai, Y., Miki, H., Yamaguchi, H. and Takenawa, T. (2000). Essential role of neural Wiskott-Aldrich syndrome protein in neurite extension in PC12 cells and rat hippocampal primary culture cells. *J. Biol. Chem.* **275**, 11987-11992.

Buccione, R., Orth, J. D. and McNiven, M. A. (2004). Foot and mouth: podosomes, invadopodia and circular dorsal ruffles. *Nat. Rev. Mol. Cell Biol.* **5**, 647-657.

Chudakov, D. M., Lukyanov, S. and Lukyanov, K. A. (2007). Tracking intracellular protein movements using photoswitchable fluorescent proteins PS-CFP2 and Dendra2. *Nat. Protoc.* **2**, 2024-2032.

Clark, E. S., Whigham, A. S., Yarbrough, W. G. and Weaver, A. M. (2007). Cortactin is an essential regulator of matrix metalloproteinase secretion and extracellular matrix degradation in invadopodia. *Cancer Res.* **67**, 4227-4235.

Condeelis, J. and Segall, J. E. (2003). Intravital imaging of cell movement in tumours. *Nat. Rev. Cancer* **3**, 921-930.

Desmarais, V., Yamaguchi, H., Oser, M., Soon, L., Mouneimne, G., Sarmiento, C., Eddy, R. and Condeelis, J. (2009). N-WASP and cortactin are involved in invadopodium-dependent chemotaxis to EGF in breast tumor cells. *Cell Motil. Cytoskeleton* **66**, 303-316.

Eckert, M. A., Lwin, T. M., Chang, A. T., Kim, J., Danis, E., Ohno-Machado, L. and Yang, J. (2011). Twist1-induced invadopodia formation promotes tumor metastasis. *Cancer Cell* **19**, 372-386.

Egeblad, M., Ewald, A. J., Askautrud, H. A., Truitt, M. L., Welm, B. E., Bainbridge, E., Peeters, G., Krummel, M. F. and Werb, Z. (2008). Visualizing stromal cell dynamics in different tumor microenvironments by spinning disk confocal microscopy. *Dis. Model Mech.* **1**, 155-167.

Entenberg, D., Wyckoff, J. B., Gligorijevic, B., Roussos, E. T., Verkhusha, V. V., Pollard, J. W. and Condeelis, J. (2011). Two laser multiphoton microscope and analysis software for multichannel intravital fluorescence imaging. *Nat. Protoc.* **6**, 1500-1520.

Even-Ram, S. and Yamada, K. M. (2005). Cell migration in 3D matrix. *Curr. Opin. Cell Biol.* **17**, 524-532.

Farina, K. L., Wyckoff, J. B., Rivera, J., Lee, H., Segall, J. E., Condeelis, J. S. and Jones, J. G. (1998). Cell motility of tumor cells visualized in living intact primary tumors using green fluorescent protein. *Cancer Res.* **58**, 2528-2532.

Fisher, K. E., Sacharidou, A., Stratman, A. N., Mayo, A. M., Fisher, S. B., Mahan, R. D., Davis, M. J. and Davis, G. E. (2009). MT1-MMP- and Cdc42-dependent signaling co-regulate cell invasion and tunnel formation in 3D collagen matrices. *J. Cell Sci.* **122**, 4558-4569.

Frederiks, W. M. and Mook, O. R. (2004). Metabolic mapping of proteinase activity with emphasis on in situ zymography of gelatinases: review and protocols. *J. Histochem. Cytochem.* **52**, 711-722.

Friedl, P. and Gilmour, D. (2009). Collective cell migration in morphogenesis, regeneration and cancer. *Nat. Rev. Mol. Cell Biol.* **10**, 445-457.

Gevrey, J. C., Isaac, B. M. and Cox, D. (2005). Syk is required for monocyte/macrophage chemotaxis to CX3CL1 (Fractalkine). *J. Immunol.* **175**, 3737-3745.

Gligorijevic, B. and Condeelis, J. C. (2009). Stretching the timescale of intravital imaging in tumors. *Cell Adh. Migr.* **3**, 313-315.

Gligorijevic, B., Kedrin, D., Segall, J. E., Condeelis, J. and van Rheenen, J. (2009). Dendra2 photoswitching through the mammary imaging window. *J. Vis. Exp.* **28**, e1278 doi: 10.3791/1278.

Kedrin, D., Gligorijevic, B., Wyckoff, J., Verkhusha, V. V., Condeelis, J., Segall, J. E. and van Rheenen, J. (2008). Intravital imaging of metastatic behavior through a mammary imaging window. *Nat. Methods* **5**, 1019-1021.

Koblinski, J. E., Ahram, M. and Sloane, B. F. (2000). Unraveling the role of proteases in cancer. *Clin. Chim. Acta.* **291**, 113-135.

Kurisu, S., Suetsugu, S., Yamazaki, D., Yamaguchi, H. and Takenawa, T. (2005). Rac-WAVE2 signaling is involved in the invasive and metastatic phenotypes of murine melanoma cells. *Oncogene* **24**, 1309-1319.

Li, A., Dawson, J. C., Forero-Vargas, M., Spence, H. J., Yu, X., Konig, I., Anderson, K. and Machesky, L. M. (2010). The actin-bundling protein fascin stabilizes actin in invadopodia and potentiates protrusive invasion. *Curr. Biol.* **20**, 339-345.

Linder, S., Nelson, D., Weiss, M. and Aepfelbacher, M. (1999). Wiskott-Aldrich syndrome protein regulates podosomes in primary human macrophages. *Proc. Natl. Acad. Sci. USA* **96**, 9648-9653.

Lorenz, M., Yamaguchi, H., Wang, Y., Singer, R. H. and Condeelis, J. (2004). Imaging sites of N-wasp activity in lamellipodia and invadopodia of carcinoma cells. *Curr. Biol.* **14**, 697-703.

Magalhaes, M., Larson, D. R., Mader, C., Bravo-Cordero, J. J., Gil-Henn, H., Oser, M., Chen, C., Koleske, A. J. and Condeelis, J. (2011). Cortactin phosphorylation regulates cell invasion through a pH dependent pathway. *J. Cell Biol.* **195**, 903-920.

Martin, T. A., Pereira, G., Watkins, G., Mansel, R. E. and Jiang, W. G. (2008). N-WASP is a putative tumour suppressor in breast cancer cells, in vitro and in vivo, and is associated with clinical outcome in patients with breast cancer. *Clin. Exp. Metastasis* **25**, 97-108.

Miki, H., Miura, K. and Takenawa, T. (1996). N-WASP, a novel actin-depolymerizing protein, regulates the cortical cytoskeletal rearrangement in a PIP2-dependent manner downstream of tyrosine kinases. *EMBO J.* **15**, 5326-5335.

Neri, A., Welch, D., Kawaguchi, T. and Nicolson, G. L. (1982). Development and biologic properties of malignant cell sublines and clones of a spontaneously metastasizing rat mammary adenocarcinoma. *J. Natl. Cancer Inst.* **68**, 507-517.

Oser, M., Yamaguchi, H., Mader, C. C., Bravo-Cordero, J. J., Arias, M., Chen, X., Desmarais, V., van Rheenen, J., Koleske, A. J. and Condeelis, J. (2009). Cortactin regulates cofilin and N-WASp activities to control the stages of invadopodium assembly and maturation. *J. Cell Biol.* **186**, 571-587.

Oser, M., Mader, C. C., Gil-Henn, H., Magalhaes, M., Bravo-Cordero, J. J., Koleske, A. J. and Condeelis, J. (2010). Specific tyrosine phosphorylation sites on cortactin regulate Nck1-dependent actin polymerization in invadopodia. *J. Cell Sci.* **123**, 3662-3673.

Oser, M., Dovas, A., Cox, D. and Condeelis, J. (2011). Nck1 and Grb2 localization patterns can distinguish invadopodia from podosomes. *Eur. J. Cell Biol.* **90**, 181-188.

Packard, B. Z., Artym, V. V., Komoriya, A. and Yamada, K. M. (2009). Direct visualization of protease activity on cells migrating in three-dimensions. *Matrix Biol.* **28**, 3-10.

Roussos, E. T., Patsialou, A. and Condeelis, J. (2011a). Chemotaxis and cancer. *Nat. Rev. Cancer* **11**, 573-587.

Roussos, E. T., Balsamo, M., Alford, S. K., Wyckoff, J. B., Gligorijevic, B., Wang, Y., Pozzuto, M., Stobezki, R., Goswami, S., Segall, J. E. et al. (2011b). Mena invasive (MenaINV) promotes multicellular streaming motility and transendothelial migration in a mouse model of breast cancer. *J. Cell Sci.* **124**, 2120-2131.

Sahai, E. (2005). Mechanisms of cancer cell invasion. *Curr. Opin. Genet. Dev.* **15**, 87-96.

Sarmiento, C., Wang, W., Dovas, A., Yamaguchi, H., Sidani, M., El-Sibai, M., Desmarais, V., Holman, H. A., Kitchen, S., Backer, J. M. et al. (2008). WASP

family members and formin proteins coordinate regulation of cell protrusions in carcinoma cells. *J. Cell Biol.* **180**, 1245-1260.

Segall, J. E., Tyerech, S., Boselli, L., Masseling, S., Helft, J., Chan, A., Jones, J. and Condeelis, J. (1996). EGF stimulates lamellipod extension in metastatic mammary adenocarcinoma cells by an actin-dependent mechanism. *Clin. Exp. Metastasis* **14**, 61-72.

Sidani, M., Wyckoff, J., Xue, C., Segall, J. E. and Condeelis, J. (2006). Probing the microenvironment of mammary tumors using multiphoton microscopy. *J. Mammary Gland Biol. Neoplasia* **11**, 151-163.

Sloane, B. F., Sameni, M., Podgorski, I., Cavallo-Medved, D. and Moin, K. (2006). Functional imaging of tumor proteolysis. *Annu. Rev. Pharmacol. Toxicol.* **46**, 301-315.

Snapper, S. B., Takeshima, F., Anton, I., Liu, C. H., Thomas, S. M., Nguyen, D., Dudley, D., Fraser, H., Purich, D., Lopez-Ilasaca, M. et al. (2001). N-WASP deficiency reveals distinct pathways for cell surface projections and microbial actin-based motility. *Nat. Cell Biol.* **3**, 897-904.

Stradal, T. E., Rottner, K., Disanza, A., Confalonieri, S., Innocenti, M. and Scita, G. (2004). Regulation of actin dynamics by WASP and WAVE family proteins. *Trends Cell Biol.* **14**, 303-311.

Takenawa, T. and Suetsugu, S. (2007). The WASP-WAVE protein network: connecting the membrane to the cytoskeleton. *Nat. Rev. Mol. Cell Biol.* **8**, 37-48.

Tolde, O., Rosel, D., Vesely, P., Folk, P. and Brabek, J. (2011). The structure of invadopodia in a complex 3D environment. *Eur. J. Cell Biol.* **89**, 674-680.

Wang, W., Wyckoff, J. B., Frohlich, V. C., Oleynikov, Y., Huttelmaier, S., Zavadil, J., Cermak, L., Bottinger, E. P., Singer, R. H., White, J. G. et al. (2002). Single cell behavior in metastatic primary mammary tumors correlated with gene expression patterns revealed by molecular profiling. *Cancer Res.* **62**, 6278-6288.

Wang, W., Goswami, S., Sahai, E., Wyckoff, J. B., Segall, J. E. and Condeelis, J. S. (2005). Tumor cells caught in the act of invading: their strategy for enhanced cell motility. *Trends Cell Biol.* **15**, 138-145.

Wolf, K., Wu, Y. I., Liu, Y., Geiger, J., Tam, E., Overall, C., Stack, M. S. and Friedl, P. (2007). Multi-step pericellular proteolysis controls the transition from individual to collective cancer cell invasion. *Nat. Cell Biol.* **9**, 893-904.

Wyckoff, J. B., Jones, J. G., Condeelis, J. S. and Segall, J. E. (2000a). A critical step in metastasis: in vivo analysis of intravasation at the primary tumor. *Cancer Res.* **60**, 2504-2511.

Wyckoff, J. B., Segall, J. E. and Condeelis, J. S. (2000b). The collection of the motile population of cells from a living tumor. *Cancer Res.* **60**, 5401-5404.

Wyckoff, J. B., Gligorijevic, B., Entenberg, D., Segall, J. E. and Condeelis, J. (2010). High-resolution multiphoton imaging of tumors in vivo. In *Live Cell Imaging: A Laboratory Manual* (ed. D. L. Spector and R. D. Goldman), pp. 441-461. New York: CSHL Press, Cold Spring Harbor.

Xue, C., Wyckoff, J., Liang, F., Sidani, M., Violini, S., Tsai, K. L., Zhang, Z. Y., Sahai, E., Condeelis, J. and Segall, J. E. (2006). Epidermal growth factor receptor overexpression results in increased tumor cell motility in vivo coordinately with enhanced intravasation and metastasis. *Cancer Res.* **66**, 192-197.

Yamaguchi, H. and Condeelis, J. (2007). Regulation of the actin cytoskeleton in cancer cell migration and invasion. *Biochim. Biophys. Acta* **1773**, 642-652.

Yamaguchi, H., Miki, H. and Takenawa, T. (2002). Neural Wiskott-Aldrich syndrome protein is involved in hepatocyte growth factor-induced migration, invasion, and tubulogenesis of epithelial cells. *Cancer Res.* **62**, 2503-2509.

Yamaguchi, H., Lorenz, M., Kempiak, S., Sarmiento, C., Coniglio, S., Symons, M., Segall, J., Eddy, R., Miki, H., Takenawa, T., et al. (2005a). Molecular mechanisms of invadopodium formation: the role of the N-WASP-Arp2/3 complex pathway and cofilin. *J. Cell Biol.* **168**, 441-452.

Yamaguchi, H., Wyckoff, J. and Condeelis, J. (2005b). Cell migration in tumors. *Curr. Opin. Cell Biol.* **17**, 559-564.

Zicha, D., Allen, W. E., Brickell, P. M., Kinnon, C., Dunn, G. A., Jones, G. E. and Thrasher, A. J. (1998). Chemotaxis of macrophages is abolished in the Wiskott-Aldrich syndrome. *Br. J. Haematol.* **101**, 659-665.